PERGAMON

Quaternary International 101–102 (2003) 169–177

Implications of distributed crustal deformation for exhumation in a portion of a transpressional plate boundary, Western Transverse Ranges, Southern California

Andrew Meigs[a,*], Doug Yule[b], Ann Blythe[c], Doug Burbank[d]

[a] Department of Geosciences, Oregon State University, 104 Wilkinson Hall, Corvallis, OR, 97330, USA
[b] Department of Geological Sciences, California State University, Northridge, CA, 91330-8266, USA
[c] Department of Earth Sciences, University of Southern California, Los Angeles, CA, 90089-0740, USA
[d] Department of Geological Sciences, University of California, Santa Barbara, CA, 93106-9630, USA

Abstract

Spatial and temporal patterns of exhumation are inextricably linked to patterns of crustal deformation because crustal deformation drives rock uplift. A new interpretation of a segment of the Pacific-North America transpressional plate boundary in southern California is analyzed in the context of crustal shortening, rock uplift, and exhumation. Deformation is partitioned between two structural anticlinoria formed above thrust faults that root into a mid-crustal décollement. The southern anticlinorium began growing after 5 Ma and is characterized by almost no topographic expression, rock uplift of $\sim$3 km, and exhumation of $<$1.2 km. Deposition in the Los Angeles basin on the south generally kept pace with growth of this anticlinorium. In contrast, the northern anticlinorium is younger, has a significant topographic expression, rock uplift of 2.5–4.0 km, and exhumation of $\sim$1.5–2 km. On-going surface uplift above the northern anticlinorium is suggested by the mismatch between the magnitude of rock uplift relative to the exhumation. These data emphasize that the distribution of deformation between faults in the upper and middle crust, crustal root formation in the lower crust, and flexural subsidence are primary controls of patterns of exhumation, which together dictate net surface uplift in active orogenic belts.

1. Introduction

Crustal deformation, exhumation, and topography are closely linked in active orogenic belts. Rock uplift is principally controlled by the distribution of faults, fault geometry, and fault slip rates. Exhumation is dictated by spatial and temporal variations in climate and erosional process acting over the region of rock uplift. Topographic change and the topographic signature of an orogenic belt depend on the magnitude, distribution, and coupling of rock uplift and exhumation (Molnar and England, 1990; Whipple et al., 1999). A contractional orogenic belt, for example, characterized by some value of internal shortening and thickening, may have distinctly different patterns of exhumation depending on how that internal deformation is accommodated (Fig. 1). Shortening that is concentrated on a single fault (Fig. 1a), results in rock uplift and associated exhumation that will be greater, for the same topography, than if the shortening is accommodated by two faults (Fig. 1b and c). Conceptually, therefore, patterns of exhumation depend on patterns and characteristics of active faults within the orogen.

An example of this coupling is presented for a portion of the western Transverse Ranges in southern California. The western Transverse Ranges have developed as the consequence of transpressional motion and block rotation in the "Big Bend" region of the San Andreas fault (Fig. 2) (Luyendyk, 1991). In detail, oblique reverse faulting on west-trending faults marks crustal deformation in the Transverse Ranges (Crook et al., 1987). Contractional deformation has resulted because the northwestward motion of the Peninsular Ranges relative to North America is greater rate than the motion of the Transverse Ranges relative to North America (Molnar and Gipson, 1994). Contractional

*Corresponding author. Tel.: +1-541-737-1214; fax: +1-541-737-1200.

E-mail addresses: meigsa@geo.orst.edu (A. Meigs), j.d.yule@csun.edu (D. Yule), blythe@usc.edu (A. Blythe), burbank@crustal.ucsb.edu (D. Burbank).

1040-6182/02/$ - see front matter © 2002 Elsevier Science Ltd and INQUA. All rights reserved.
PII: S1040-6182(02)00099-X

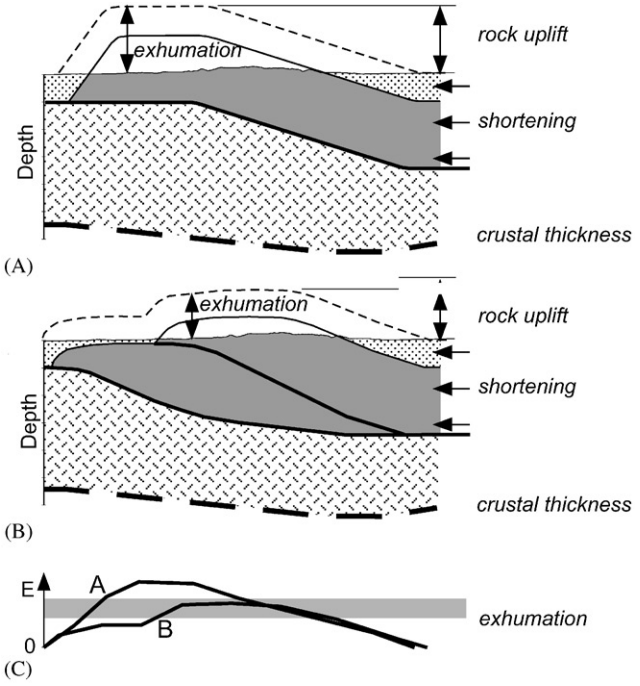

Fig. 1. Conceptual model of differences in exhumation (C) for crustal-scale cross sections with a single thrust fault (A) and two thrust faults (B) with equivalent shortening and surface topography. Rock uplift is given by the height of the dashed marker relative to its regional elevation outside the deformed region. (C) Exhumation (E) is measured as the difference between the structural relief of the dashed bedrock marker (rock uplift) and the earth 's surface in (A) and (B). The gray band in (C) represents schematically the range in the amount of material that must be removed in order that a cooling age derived from a thermochronometer have an age that corresponds with the period of shortening and exhumation depicted in A or B. Topographic effects on isotherms are ignored. Note that for the same shortening, the rock uplift and exhumation are lower for the two-fault case (B) because the deformation and associated vertical uplift of rocks is more broadly distributed.

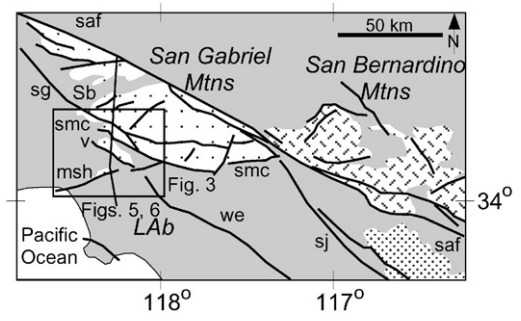

Fig. 2. Location map for the western Transverse Ranges in southern California. A box indicates the location of the map in Fig. 3. A line indicates the cross section in Figs. 5 and 6. Major faults include the San Andreas (saf), the San Jacinto (sj), the Whittier-Elsinore (we), the Malibu-Santa Monica-Hollywood (msh), the Verdugo (v), the San Gabriel (sg), and the Sierra Madre-Cucamonga (smc). Depositional basins are the Los Angeles and Soledad basins (LAb and Sb, respectively). Basement rocks of the San Gabriel Mountains (open stipple), the San Bernardino Mountains (diagonal hatch), and the Peninsular Ranges (tight stipple) are differentiated. The San Gabriel and San Bernardino Mountains are part of the Transverse Ranges.

deformation within the Transverse Ranges has persisted for roughly 5–7 Myr given the age of growth strata on the limbs of contractional folds (Wright, 1991; Schneider et al., 1996). Prior to 7 Ma, transtensional deformation dominated (Ingersoll and Rumelhart, 1999).

In this paper we reconcile marked differences between rock uplift and relatively modest exhumation across the southern front of the Western Transverse Ranges (south of the San Gabriel fault; Figs. 2 and 3). Upper crustal structure is constrained with new geologic mapping, published data including bedrock maps, surficial geologic maps, and cross sections. A new crustal-scale cross section is presented, which combines these data with geophysical data and crustal seismicity in order to relate the structural geometry to the crustal-scale accommodation of shortening. Exhumation magnitude is constrained by the thickness of strata eroded from the crests of the major structures and by fission-track and (U–Th)/He thermochronometry. The signal of deformation and rock uplift in the records of exhumation south of the San Gabriel fault is dampened because shortening is distributed between two structural anticlinoria that involve the middle and upper crust. Although large surface uplift might be expected due to the mismatch between rock uplift and exhumation, the magnitude of surface uplift is apparently suppressed by a combination of compensation by creation of the lower crustal root and flexural subsidence. This analysis provides new insight into the key role that structural control plays in the interpretation of spatial and temporal patterns of exhumation from thermochronometric data.

2. Crustal structure

Two broad structural highs characterize the surface expression of the major structures in the study area (Fig. 3). On the south, the southern anticlinorium extends from the central trough of the Los Angeles basin to the Verdugo fault (Fig. 4a). The northern anticlinorium includes the region from the hanging wall of the Verdugo fault to the San Gabriel Fault on the north (Figs. 4b and c). The western San Gabriel Mountains block comprises the remainder of the cross section north of the San Gabriel fault to the San Andreas fault. The pattern of Pliocene deformation of the western San Gabriel Mountains block is unclear because sedimentary strata are not preserved south of the Soledad basin (Fig. 2). However, thermochronologic data indicate that less than 1.7 km of exhumation has occurred in this part of the San Gabriel Mountains since 15 Ma (Blythe et al., 2000, in press). The pattern of rock uplift and exhumation in the Transverse Ranges south of the San Gabriel fault are delineated in this paper.

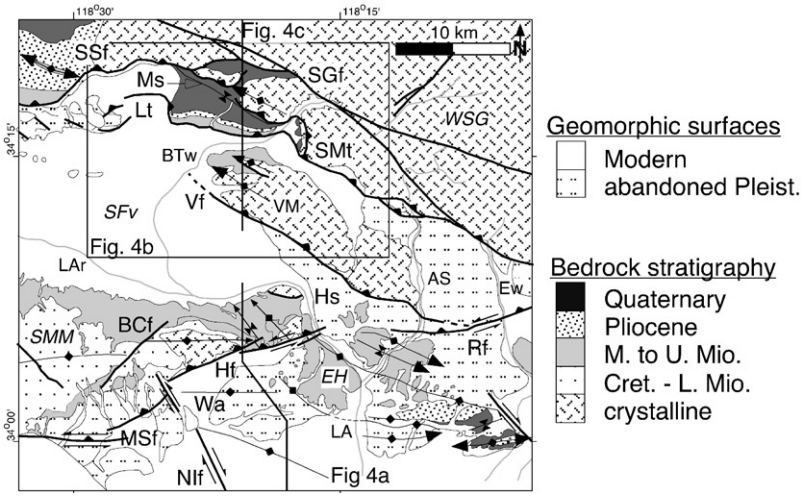

Fig. 3. Bedrock geologic map of the study area. The southern anticlinoria extends across the eastern Santa Monica Mountains and Elysian Hills (cross-section in Fig. 4A). The northern anticlinoria extends from the eastern San Fernando Valley and Verdugo Mountains to the San Gabriel Mountains (map (Fig. 4b) and cross section (Fig. 4c)). Key folds are the Wilshire arch (Wa) and the Merrick syncline (Ms). Major faults include the Newport-Englewood (NIf), Malibu-Santa Monica (MSf), Hollywood (Hf), Hollister (Hs), Benedict Canyon (BCf), Raymond (Rf), Verdugo (Vf), Lakeview (Lt), Sierra Madre (SMt), Santa Susana (SSf), and San Gabriel (SGf). Drainages include the Los Angeles River (LAr), Big Tujunga Wash (BTw), Arroyo Seco (AS), and Eaton Wash (Ew). Geographic locations include Los Angeles (LA), the Elysian Hills (EH), the Santa Monica Mountains (SMM), the Verdugo Mountains (VM), the San Fernando Valley (SFv), and the western San Gabriel Mountains (WSG). Map sources from Crook et al. (1987), Dibblee (1989, 1991a–c), Hill (1930), Hoots (1931), and Oakeshott (1958).

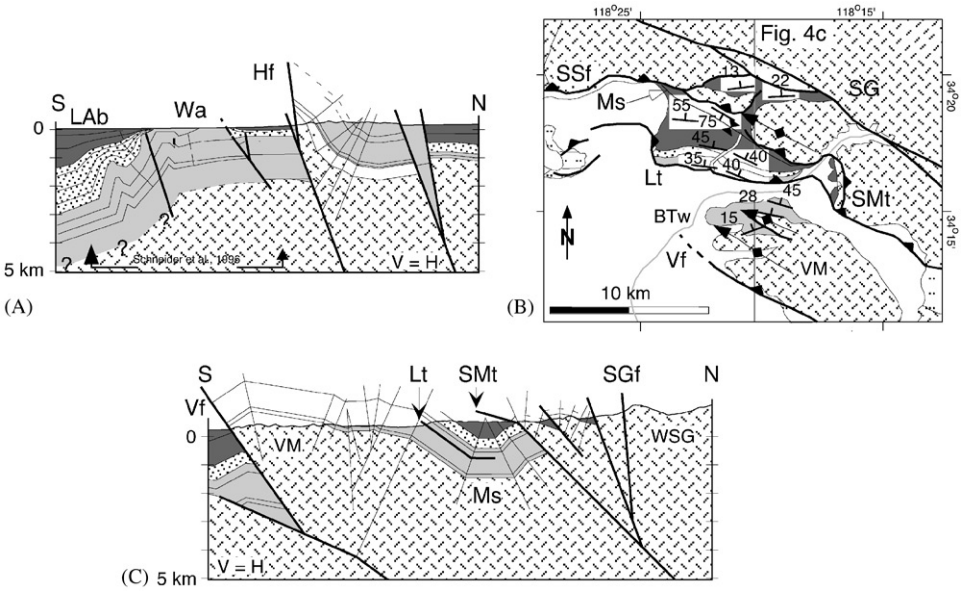

Fig. 4. (A) Cross section across the southern anticlinoria. Section to the north and south of the Wilshire arch (Wa) in the Los Angeles basin (LAb) after Schneider et al. (1996). The two faults to the north of the Hollywood fault (Hf) are projections of the Benedict Canyon and Hollister faults on to the line of section (BCf, Hs, respectively). (B) Map and structural data from the northeastern Verdugo Mountains and southern San Gabriel Mountains to the north and south of the Big Tujunga Wash, respectively. (C) Cross section across the northern anticlinoria. Hanging wall and footwall of the Vf are from Tsutsumi and Yeats (1999). Abbreviations and symbols are defined in Fig. 3.

2.1. Southern anticlinorium

The southern anticlinorium is a broad structural high, the crest of which is cut by the Hollywood fault (Fig. 4a). To the south of the Hollywood fault the anticlinorium has almost no topographic signature but has nearly 3 km of structural relief (Schneider et al., 1996). A south-facing monocline with a steeply south-dipping south limb and a flat crest defines the overall structure. Offset fold axes and stratigraphic contacts provide evidence of the long-term left oblique–reverse displacement on the Hollywood fault (Meigs and Oskin, in press). Dip- and strike-slip offsets are nearly equal across the fault. Hanging wall structure consists of a

syncline that is cut by faults with unknown sense and magnitude of separation. The north flank of the southern anticlinorium comprises a gently north-dipping panel that projects under the San Fernando Valley to the north (Tsutsumi and Yeats, 1999). Pliocene strata are preserved across the anticlinorium except on the crest of the Wilshire Arch and the hanging wall of the Hollywood fault where these strata are eroded. Growth stratal geometries in Pliocene and younger sediments document growth of the south-facing monocline after 5 Ma (Fig. 4a) (Schneider et al., 1996).

2.2. Northern anticlinorium

A compound structure characterizes the northern anticlinorium (Fig. 4c). Between the Verdugo fault on the south and the Sierra Madre thrust on the north, the structure consists of an anticline–syncline pair. Bedding dips in Miocene strata in the northwestern Verdugo Mountains and to the north across the Big Tujunga River are similar and there is no apparent stratigraphic duplication across the Lakeview thrust (Fig. 4b). The Lakeview thrust ruptured in the 1971 San Fernando earthquake (Kamb et al., 1971; Sharp, 1975). Dips on the surface ruptures are similar to the dip of Miocene beds, which, in conjunction with the lack of stratigraphic duplication across the fault, support an interpretation of the surface ruptures as secondary rupture of flexural slip faults (Tsutsumi and Yeats, 1999). Younger units are concordant with older deposits on the limbs of the Merrick syncline. These beds and the synclinal axial trace are cut by the Sierra Madre thrust (Figs. 4b and c). Hanging wall structure of the Sierra Madre thrust consists of two short wavelength anticlines marked by folded Quaternary strata unconformably overlying crystalline basement and separated by a small-displacement thrust (Fig. 4c). Fault strands representing the San Gabriel fault zone cut the north flank of the northern anticlinorium. The conformable stratigraphic section in the Merrick syncline suggests the anticline in the Verdugo Mountains developed during or after accumulation of the Quaternary sediments. In contrast, the missing Miocene and Pliocene strata in the hanging wall anticline of the Sierra Madre thrust indicate compound growth of the folds on the northern side of the anticlinorium. Coseismic rupture of flexural slip faults (Lakeview thrust), folding of Quaternary strata, and truncation of the Merrick synclinal axial trace attest to the ongoing, distributed deformation within the anticlinorium.

3. Shortening

Crustal shortening was calculated using the line length of the contact between Miocene and Pliocene strata (Fig. 5). This stratigraphic level is appropriate for line length balancing because it marks the end of a lull in deformation between the earlier transtensional deformational regime and the present contractional regime (Wright, 1991; Schneider et al., 1996; Tsutsumi and Yeats, 1999;). Well, data suggest that the top of the Miocene section (Delmontian strata (6.5–4.95 Ma), Blake, 1991) is continuous across the northern Los Angeles basin and San Fernando Valley and largely buried topography developed during the preceding period of transtensional deformation (Schneider et al., 1996; Tsutsumi and Yeats, 1999). Regional pin lines located in the northern edge of the Los Angeles basin on the south and at the axis of the Merrick syncline on the north form the frame of reference of the restoration (Fig. 5). The present, horizontal distance between these pin lines is ~28.5 km, whereas the line length of the base of the Pliocene section is ~35.6 km. Thus, the base of the Pliocene is shortened by approximately 7.1 km. Pliocene strata are not preserved between the Hollywood fault and faults on the southern edge of the San Fernando Valley and across the Verdugo Mountains. The structural geometry where these strata are eroded was constrained by projection of dip data from lower structural levels and from along-strike. Line length of the base-Pliocene marker across the two eroded hanging wall cutoffs thus represents a minimum estimate.

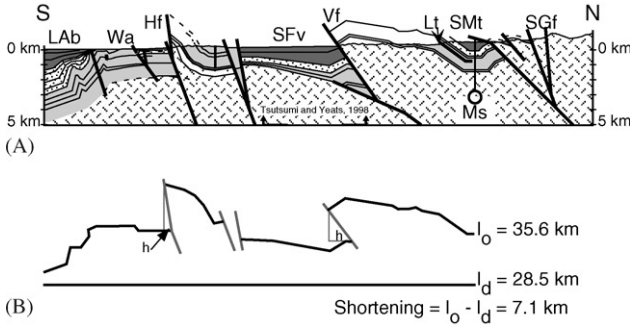

Fig. 5. (A) Upper crustal cross section across the two anticlinorium. (B) Shortening calculated from the horizontal distance (l_d) between pin lines in the Merrick syncline and in the Los Angeles basin based on the line length of the base of Pliocene strata (dense stipple in A) (l_o).The minimum horizontal component of motion due to fault displacement is indicated by h. Abbreviations and symbols are defined in Fig. 3.

4. Exhumation

Exhumation was estimated in two different ways. To the south of the San Gabriel fault, the thickness of strata missing across the crests of anticlines and structural highs provides a measure of exhumation. Stratigraphic thickness was established at the axes of nearby synclines, which are assumed to undergo negligible uplift and erosion during folding. Exhumation was measured as

the difference between the projection of the highest stratigraphic level and the ground surface. Fission-track and (U–Th)/He cooling ages of apatite from bedrock samples provided estimates of exhumation in San Gabriel Mountains north of the Sierra Madre thrust fault (for complete reporting of methods, data, and results see Blythe et al., 2000, in press).

4.1. Southern anticlinorium

The southern anticlinorium has almost no surface expression, except on the north flank in the eastern Santa Monica Mountains (Fig. 4a). Accumulation of more than 3 km of sediment accompanied growth of the anticlinorium as a result of its development adjacent to the subsiding central trough of the Los Angeles basin (Wright, 1991; Schneider et al., 1996). Sedimentation largely kept pace with uplift during growth, with the exception of the structural crest (Figs. 4a and 5). Thin Quaternary sediments unconformably overlie lower Upper Miocene strata (Schneider et al., 1996), which implies ~1.2 km of section have been eroded across the Wilshire arch. Growth strata deposited between 4.95 and 2.5 Ma are thinned considerably at the crest, but internal growth stratigraphic geometries suggest they may have been continuous across the crest of the fold, implying that 1.2 km of section were removed after 2.5 Ma (Fig. 6a).

Additional exhumation across the crest is associated with uplift of the hanging wall of the Hollywood fault. Removal of the complete stratigraphic section is reflected by the exposure of basement rocks (Fig. 5). Rocks younger than Miocene are not exposed in the eastern Santa Monica Mountains (Hoots, 1931; Dibblee, 1982; Meigs and Oskin, in press), which implies that the 2 km peak in exhumation in the hanging wall may be a minimum (Fig. 6a). Subsurface data across the north flank of the anticlinorium underlying the southern San Fernando Valley demonstrate that the Pliocene and Quaternary sections are thin, but concordant (Tsutsumi and Yeats, 1999). Unconformities in the section beneath the San Fernando Valley would thus represent either non-deposition or erosion without substantial tilting. Existing subsurface data and age control are insufficient to differentiate between these two possibilities.

4.2. Northern anticlinorium

In contrast to the southern anticlinorium, the northern anticlinorium is characterized by a greater amount

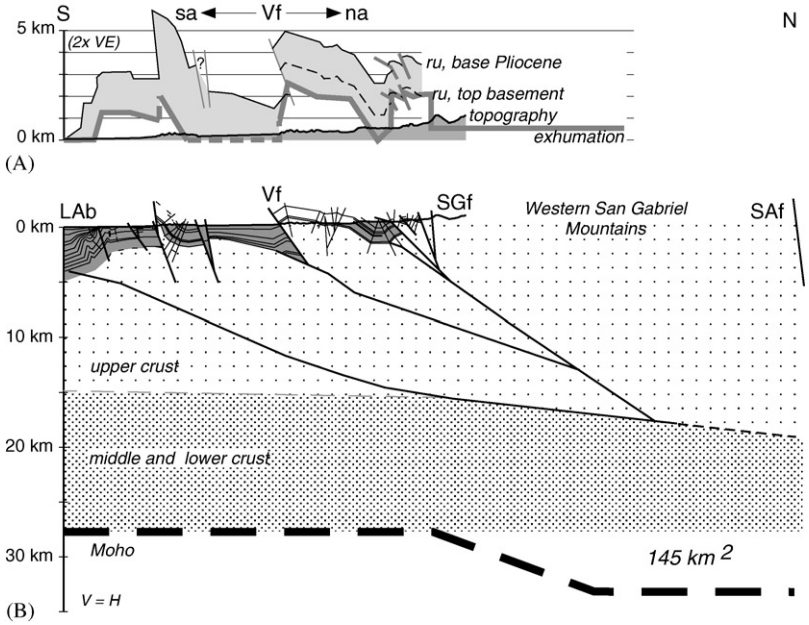

Fig. 6. (A) Exhumation, rock uplift (ru), and present topography (2 × vertical exaggeration). Exhumation to the south of the San Gabriel fault (SGf) is given by the difference between the elevation of the base of the Pliocene and the topographic surface. To the north of the SGf, Pliocene-Recent exhumation is estimated from exhumation rates derived from apatite fission-track and (U–Th)/He thermochronometric data (Blythe et al., 2000; in press). Rock uplift is plotted for the base of the Pliocene relative to depth to the base of the Pliocene in the Los Angeles basin (Lab) on the south (solid line). Rock uplift values for the northern anticlinorium are reported relative to the depth to the Pliocene in the footwall of the Verdugo fault (Vf) in the text. North of the Vf, ru is also reported for the top of the basement relative to the depth of basement in the footwall of the Vf (dashed line). Predicted surface uplift is the difference between ru and exhumation and is indicated by the shaded region. SA and NA denote the southern and northern anticlinoria, respectively. (B) Crustal-scale cross section across southern and northern anticlinoria. Fault topology at depth is interpreted from bedrock surface and shallow subsurface data, crustal seismicity, and geophysical data. Sediments (dark shade), basement of the upper (open dots), and the middle-lower crust (tight dots), are differentiated. The mid-crustal detachment depth, approximate depth of the boundary between the upper and middle-lower crust, and Moho depth are after Fuis et al. (2001).

of structural relief and exhumation (Figs. 4c and 6). Miocene and younger sediments are exposed only on the northeastern flank of the Verdugo Mountains, the Merrick syncline, and as a thin veneer above basement-cored anticlines in the hanging wall of the Sierra Madre thrust. A pre-contractional ~2 km stratigraphic thickness overlying these structures is given by the thickness of these units at the axis of the Merrick syncline (Fig. 4c). Basement rocks are exposed throughout much of the Verdugo Mountains (Fig. 3). Projection of dip data and fold geometry onto the line of section allows estimation of a minimum of 2 km of exhumation in the Verdugo Mountains, which must decrease to 0 km at the axis of the Merrick syncline on the north (Fig. 6). Uplift and erosion across the fold expressed in the Verdugo Mountains apparently postdates deposition of the Saugus Formation (2.3–0.5 Ma, Levi and Yeats, 1993), given that these strata are depositionally concordant with Pliocene and older sediments preserved in the south limb of the Merrick syncline (Figs. 4b and c). Less than 2 km of exhumation since 7 Ma is suggested by the cooling ages and cooling history of apatite samples from the region between the Sierra Madre and San Gabriel faults (the so-called Tujunga block of Blythe et al., 2000). A folded unconformity between discontinuous Saugus Formation and basement rocks requires that at least 2 km of section is missing from the hanging wall of the Sierra Madre thrust. A period of uplift and erosion predating deposition, folding, and uplift of the deposits of the Saugus Formation is suggested by the unconformable relationships.

4.3. Western San Gabriel Mountains

Only basement rocks are exposed in the western San Gabriel Mountains (the portion of the mountains to the north of the San Gabriel fault), in the vicinity of the line of section (Figs. 2 and 3). Magnitude of exhumation along this portion of the section is based on cooling ages of apatite determined using fission-track and (U–Th)/He thermochronometry. Details of the thermochronometric data including fission-track and (U–Th)/He methods, raw data, sample location and density, and age determinations can be found in Blythe et al. (2000, in press). It is sufficient, for the purposes of this paper, to summarize how the magnitude of exhumation and exhumation rate were determined from these data. Fission-track ages record the time at which a sample cooled below ~110°C (Gleadow et al., 1986; Green et al., 1986), whereas (U–Th)/He ages record cooling below ~70°C (Farley, 2000). Tertiary cooling ages are revealed by both methods for samples from the western San Gabriel Mountains to the north and northeast of the San Gabriel fault (Fig. 3). Because the cooling ages range from ~16 to 63 Ma, the ages do not constrain directly the cooling history related to the period of contractional deformation described in this study. Fission-track length distributions can be inverted for a sample's history of cooling below ~110°C (Green et al., 1989); however, because fission-track annealing, which shortens track length, occurs as samples pass through the partial annealing zone of apatite, between ~110°C and 60°C (Gleadow and Fitzgerald, 1987). Models of cooling history for appropriate samples suggest that the samples had cooled to ~80°–50°C by ≈15 Ma (Blythe et al., 2000, in press). The minimum amount of rock exhumed to reveal these samples at the surface (1.7 km) was approximated by converting the lower bound on temperature (50°C) to an equivalent depth using an assumed geothermal gradient of 30°C/km. A mean exhumation rate of 0.11 mm/yr since ~15 Ma was inferred from this approximation. If the exhumation rate has been steady since 15 Ma, ~0.6 km of exhumation has occurred between the San Gabriel and San Andreas faults since 5 Ma (Fig. 6a).

5. Discussion

Shortening and exhumation are closely coupled for both the southern and northern anticlinoria (Fig. 6). Growth of the southern anticlinorium was accompanied by nearly continuous sedimentation, the rate of which was close to the rate of crestal uplift. Subaerial exposure and erosion are likely to be significant only after 2.5 Ma, given the thickness and discontinuous preservation of older Pliocene strata across the crest of the anticlinorium (Schneider et al., 1996). Although as much as 1.2 km of section is missing across the Wilshire arch (Fig. 4a), geometry of the growth sequence and the lack of a topographic expression of the fold imply that this missing thickness reflects a combination of erosion and non-deposition. The rate of rock uplift is given by the structural relief across the anticlinorium divided by the duration of fold growth (~0.6 km/Myr, 3 km, 5 Myr, respectively) and is greater than rate of exhumation (1.2 km/5 Myr = 0.24 km/Myr). Surface uplift and development of a topographic expression are predicted by this mismatch, but may have been suppressed by basin subsidence at nearly the same rate as crestal uplift (Schneider et al., 1996). Thus, the load driven subsidence, because it moves rock in an opposite sense relative to fold crestal uplift, effectively diminished the net rock uplift across the anticlinorium. It is only above the high-angle Hollywood fault that topography has developed (Figs. 6a). The different topographic expression for this part of the anticlinorium highlights the importance of fault angle on rock uplift rate (Fig. 6).

Growth and exhumation of the northern anticlinorium is more complex. A simple uplift and erosion history is implied for that part of the anticlinorium

represented by the Verdugo Mountains. Structural arguments suggest that folding was initiated concurrent with or after deposition of the Saugus Formation. Maximum structural relief of the hanging wall of the Verdugo fault relative to the footwall is ~2.5 km (Fig. 4c), which implies a minimum rock uplift rate of 1.1 km/Myr, assuming uplift began after 2.3 Ma (the age of the base of the Saugus Formation Levi and Yeats, 1993). Exhumation is ~2 km (Fig. 6a), implying that the minimum exhumation rate is 0.9 km/Myr and that ~0.5 km of surface uplift has occurred since 2.3 Ma. Mean elevation along the line of section is ~330 m, although it is higher to the southeast. The present mean elevation likely represents net surface uplift because the lower part of the Saugus Formation represents a transition from marine to non-marine deposition (Oakeshott, 1958; Levi and Yeats, 1993), and because it is consistent with the difference between rock uplift and exhumation. If uplift of the Verdugo Mountains is younger than the top of the Saugus Formation (0.5 Ma), the rates reported above would be higher by roughly a factor of 5.

To the north, in the hanging wall of the Sierra Madre thrust, a more complex uplift and exhumation history is implied by the unconformity between the Saugus Formation and basement (Fig. 4b). Determining when the deformation and exhumation occurred in time depends on the age of the Saugus Formation. Structural data suggest that strata overlying the basement are roughly equivalent to strata 400–500 m below the youngest strata preserved along the axial trace of the Merrick syncline (Fig. 4c). On this basis, the upper Saugus Formation is the most likely stratigraphic equivalent to these deposits. Initial uplift on the northern edge of the anticlinorium is inferred to have occurred prior to 0.5 Ma and resulted in the removal of at least 1.5 km of pre-Saugus sedimentary deposits (Fig. 6a). The first appearance of locally derived clasts due to the uplift of the hanging wall of the Santa Susana thrust, the along-strike correlative of the Sierra Madre thrust (Fig. 3), is constrained to ~0.7 Ma (Levi and Yeats, 1993). If this age of initiation applies to the northern edge of the anticlinorium in the study area, an exhumation rate of 2.1 km/Myr is suggested.

Folding of locally preserved Saugus Formation on basement implies that deformation shifted between structures, that sedimentation rates periodically exceeded uplift rates, or that both occurred during growth of the northern anticlinorium. Structural relief (rock uplift) is bracketed between 2.5 and 4.0 km. These estimates of structural relief reflect the minimum uplift of basement in the hanging wall of the Sierra Madre thrust relative to basement in the footwall of the Sierra Madre or Verdugo thrusts, respectively. The uncertainty reflects the absence of a marker in the hanging wall to correlate with a footwall unit. Maximum rock uplift rates of 3.6–5.7 km/Myr are implied for initiation at ~0.7 Ma. A positive surface uplift rate is suggested by the discrepancy between structural relief and magnitude of exhumation, regardless of the age of initiation. Mean elevation between the Sierra Madre thrust and San Gabriel fault (Figs. 3 and 6) is ~860 m (Blythe et al., 2000). The present mean elevation across the northern anticlinorium is roughly half the mean elevation implied by the difference between the rock uplift and exhumation (Fig. 6), which may reflect flexural subsidence due to loading.

If the faults at the base of the anticlinoria in the upper crust root into a mid-crustal décollement as suggested most recently by the LARSE seismic reflection profiles (Fuis et al., 2001), a crustal root in the lower crust must have developed to maintain a balance between shortening above and below the décollement (Fig. 6b). The cross-sectional area of the lower crustal root and the sum of the change in area due to shortening plus the area of rock missing due to exhumation serve as order-of-magnitude estimates of thickening at two different levels in the crust. For a mid-crustal décollement at ~18 km (Fuis et al., 2001), and shortening of ~7 km (Fig. 5), the area change due to crustal thickening along the line of section is 126 km^2. The missing area representing exhumation between the Los Angeles basin on the south and the San Gabriel fault on the north is 32 km^2 (Fig. 6).

The area of the lower crustal root south of the San Andreas fault is approximately 145 km^2. Significant uncertainty is associated with these estimations due to (1) the erosion of hanging wall cutoffs (shortening), (2) the projection of constant-thickness beds across eroded areas (exhumation), (3) the emphasis on the dip-slip component of fault displacement given that oblique slip likely characterizes the net slip on the two fault systems, and (4) the projection of the position and size of the crustal root ~30 km from the LARSE profile along-strike to the northwest on to the line of section. It is intriguing, however, that these rough estimates of change in cross-sectional area due to shortening, thickening, and erosion of the upper and middle crust (158 km^2) nearly match the estimated area of thickened lower crust (145 km^2). If broadly correct, the near balance between the changes in area in the upper and lower crust suggests that the estimates of shortening and exhumation are reasonable. It also suggests that the amount of shortening and thickening between the San Gabriel and San Andreas faults in the western San Gabriel Mountains is relatively small in comparison with that documented to the south. As illustrated by this analysis, substantial shortening can be absorbed by distributed deformation without significant exhumation, which has implications for the interpretation of exhumation records in general. The example presented here indicates that, despite ~7 km of shortening

measured across the southern flank of the western Transverse Ranges, less than 2.5 km of exhumation has occurred anywhere in the line of section. The absence of an interpretable pattern of exhumation related to the pattern of crustal deformation in the low temperature thermochronometric data over the past ~ 5 Myr can be attributed to the distributed nature of the deformation. Thus, interpretation of the spatial and temporal patterns of exhumation from such data sets is limited without adequate structural control. Surface uplift, the other potential outcome of crustal shortening and thickening may also be subdued because the majority of shortening may be absorbed by formation and isostatic compensation of a lower crustal root and/or flexural subsidence due to loading.

6. Conclusions

A new interpretation of a segment of the Pacific-North America transpressional plate boundary in southern California illustrates the close relationship between spatial and temporal patterns of exhumation and crustal deformation. Deformation within the boundary region is partitioned between two structural anticlinoria formed above thrust faults that root into a mid-crustal décollement. The southern anticlinorium began growing after 5 Ma and is characterized by almost no topographic expression, rock uplift of ~ 3 km, and exhumation of < 1.2 km. The northern anticlinorium is likely younger, has a significant topographic expression, rock uplift of 2.5–4.0 km, and exhumation of ~ 1.5–2 km. Whereas the southern anticlinorium lacks a significant surface expression because sedimentation generally kept pace with rock uplift, a discrepancy between the measured rock uplift and exhumation implies on-going surface uplift above the northern anticlinorium. Low-temperature thermochronometric data do not directly record a Pliocene and younger cooling event. Cross-sectional area changes in the upper crust due to shortening are apparently balanced by the lower crustal root.

Acknowledgements

A.J.M. was supported by a Division of Geological and Planetary Sciences, California Institute of Technology Postdoctoral Fellowship and a Southern California Earthquake Center Postdoctoral Fellowship. This research was supported by the Southern California Earthquake Center and grants from the NASA Topography and Surface Change program (NASA (NAG-5-2191), NASA (NAG-5-7646)). SCEC is funded by NSF Cooperative Agreement EAR-8920136 and USGS Cooperative Agreements 14-08-0001-A0899 and 1434-HQ-97AG01718. The SCEC contribution number for this paper is 697.

References

Blake, G.H., 1991. Review of the Neogene biostratigraphy and stratigraphy of the Los Angeles basin and implications for basin evolution. In: Biddle, K.T. (Ed.), Active Margin Basins. American Association of Petroleum Geologists Memoir Tulsa 52, 135–184.

Blythe, A.E., Burbank, D.W., Farley, K.A., Fielding, E.J., 2000. Structural and topographic evolution of the central Transverse Ranges, California, from apatite fission-track,(U–Th)/He and digital elevation model analyses. Basin Research 12, 97–114.

Blythe, A.E., House, M.A., Spotila, J.A. Low-temperature thermochronology of the San Gabriel and San Bernardino Mountains, southern California: constraining structural evolution, In: Barth, A. (Ed.), Geological Society of America Special Paper in Honor of the Late Perry Ehlig. Geological Society of America, Boulder, CO, in press.

Crook Jr., R., Allen, C.R., Kamb, B., Payne, C.M., Proctor, R.J., 1987. Quaternary geology and seismic hazard of the Sierra Madre and associated faults, western San Gabriel Mountains. In: Morton, D.M., Yerkes, R.F. (Eds.), Recent Reverse Faulting in the Transverse Ranges, California. United States Geological Survey Professional Paper 1339, 27–64.

Dibblee, T.W.J., 1982. Geology of the Santa Monica Mountains and Simi Hills, southern California, In: Fife, D.L., Minch, J.A. (Eds.), Geology and Mineral Wealth of the California Transverse Ranges. South Coast Geological Society, Annual Symposium and Guidebook 10, pp. 94–130.

Dibblee, T.W., 1989. Geologic map of the Los Angeles Quadrangle, Los Angeles County, California. Dibblee Geological Foundation, DF-22, 1:24,000.

Dibblee, T.W., 1991a. Geologic map of the Beverly Hills and Van Nuys (South 1/2) Quadrangle, Los Angeles County, California. Dibblee Geological Foundation, DF-31, 1:24,000.

Dibblee, T.W., 1991b. Geologic map of the Hollywood and Burbank (South 1/2) Quadrangles, Los Angeles County, California. Dibblee Geological Foundation, DF-30, 1:24,000.

Dibblee Jr., T.W., 1991c. Geologic map of the Sunland and Burbank (north 1/2) Quadrangles, Los Angeles County, California. Dibblee Geological Foundation, DF-32, 1:24,000.

Farley, K.A., 2000. Helium diffusion from apatite: general behaviors as illustrated by Durango fluorapatite. Journal of Geophysical Research 105, 2903–2914.

Fuis, G.S., Ryberg, T., Godfrey, N.J., Okaya, D.A., Murphy, J.M., 2001. Crustal structure and tectonics from the Los Angeles basin to the Mojave Desert, southern California. Geology 29, 15–18.

Gleadow, A.J.W., Fitzgerald, P.G., 1987. Uplift history and structure of the Transantarctic Mountains: new evidence from fission track dating of basement apatites in the dry valleys area, southern Victoria land. Earth and Planetary Science Letters 82, 1–14.

Gleadow, A.J.W., Duddy, I.R., Green, P.F., Lovering, J.F., 1986. Confined fission track lengths in apatite—a diagnostic tool for thermal history analysis. Contributions to Mineralogy and Petrology 94, 405–415.

Green, P.F., Duddy, I.R., Gleadow, A.J.W., Tingate, P.R., Laslett, G.M., 1986. Thermal annealing of fission tracks in apatite: 1.—a qualitative description. Chemical Geology (Isotope Geoscience Section) 59, 237–253.

Green, P.F., Duddy, I.R., Laslett, G.M., Hegarty, K.A., Gleadow, A.J.W., Lovering, J.F., 1989. Thermal annealing of fission track in apatite: 4. Qualitative modelling techniques and extensions to geological timescales. Chemical Geology (Isotope Geoscience Section) 79, 155–182.

Hill, M.L., 1930. Structure of the San Gabriel Mountains, north of Los Angeles, California. University of California Publications, Department of Geological Sciences Bulletin 19, 137–170.

Hoots, H.W., 1931. Geology of the Eastern Part of the Santa Monica Mountains Los Angeles County, California. United States Geological Survey Professional Paper 165-C, United States Geological Survey, Washington, 51pp.

Ingersoll, R.V., Rumelhart, P.E., 1999. Three-stage evolution of the Los Angeles basin, southern California. Geology 27, 593–596.

Kamb, B., Silver, L.T., Abrams, M.J., Carter, B.A., Jordan, T.H., Minster, J.B., 1971. Pattern of faulting and nature of fault movement in the San Fernando Earthquake. In: The San Fernando, California earthquake of February 9, 1971. United States Geological Survey Professional Paper 733, pp. 41–54.

Levi, S., Yeats, R.S., 1993. Paleomagnetic constraints on the initiation of uplift on the Santa Susana fault, western Transverse Ranges, California. Tectonics 12, 688–702.

Luyendyk, B.P., 1991. A model for Neogene crustal rotations, transtension, and transpression in southern California. Geological Society of America Bulletin 103, 1528–1536.

Meigs, A.J., Oskin, M.E. Convergence, block rotation, and structural interference across the Peninsular-Transverse Ranges boundary, eastern Santa Monica Mountains, California, In: Barth, A. (Ed.), Geological Society of America Special Paper in Honor of the Late Perry Ehlig. Geological Society of America Special Paper, Geological Society of America, Boulder, CO, in press.

Molnar, P., England, P., 1990. Late Cenozoic uplift of mountain ranges and global climatic changes: chicken or egg? Nature 346, 29–34.

Molnar, P., Gipson, J.M., 1994. Very long baseline interferometry and active rotations of crustal blocks in the Western Transverse Ranges, California. Geological Society of America Bulletin 106, 594–606.

Oakeshott, G.B., 1958. Geology and mineral deposits of the San Fernando Quadrangle, Los Angeles County, California. California Divisions of Mines and Geology Bulletin 172, 147.

Schneider, C.L., Hummon, C., Yeats, R.S., Huftile, G.J., 1996. Structural evolution of the northern Los Angeles basin, California, based on growth strata. Tectonics 15, 341–355.

Sharp, R.V., 1975. Displacement on tectonic ruptures. In: Oakeshott, G.B. (Ed.), San Fernando, California earthquake of 9 February 1971. California Division of Mines and Geology Bulletin 196, pp. 187–194.

Tsutsumi, H., Yeats, R.S., 1999. Tectonic setting of the 1971 Sylmar and 1994 Northridge earthquakes in the San Fernando Valley, California. Bulletin of the Seismological Society of America 89, 1232–1249.

Whipple, K.X., Kirby, E., Brocklehurst, S.H., 1999. Geomorphic limits to climatically induced increases in topographic relief. Nature 401, 39–43.

Wright, T.L., 1991. Structural geology and tectonic evolution of the Los Angeles basin, California, In: Biddle, K.T. (Ed.), Active Margin Basins ,Vol. 52. American Association of Petroleum Geologists Memoir, pp. 35–134.